Extending the pMSSM Coverage with Gluino-Squark Simplified Models Results

Federico Ambrogi[a]

[a]*University of Vienna, Faculty of Physics, Bolzmanngasse 5, A-1090 Wien, Austria*

Abstract

The ATLAS collaboration at the Large Hadron Collider (LHC) analysed in arXiv:1508.06608 the constraints provided by the Run 1 searches, performed at 8 TeV centre-of-mass energy, on a 19-parameters realisation of the phenomenological Minimal Supersymmetric Standard Model (pMSSM). It was shown in arXiv:1707.09036 that a large fraction of the parameter space of this model can be efficiently constrained by means of simplified models spectra (SMS) results. The missed part could be potentially covered by a new class of simplified model stemming from gluino-squark associated production, producing a 3 jets plus missing energy signature in the LHC detectors. This work aims at demonstrating that by recasting existing searches with such simplified model, it is possible to extend significantly the coverage of the pMSSM-19 parameter space with simplified models results.

Contents

1. Introduction

Simplified models spectra have become the standard method for the LHC collaborations to interpret the results of their searches for Beyond the Standard Model (BSM) particles, as in the case of Supersymmetry (SUSY). The most notable benefit coming from the adoption of SMS is the drastic reduction of the large parameter spaces of full theories. SMS serve not only as a useful benchmark to design and optimize the searches, but also they can easily highlight the specific strength of each search. All of this is possible thanks to the handful of new parameters introduced by each simplified model. Moreover, only a few SUSY particle appears in each SMS, while all the remaining are considered decoupled, i.e. their masses are too large so that the production cross section at the LHC is negligible, and they do not appear as intermediate on-shell states in cascade decays.

In the case of SUSY, the masses of the of the particles, their production cross section and their decay modes are sufficient to fully characterise the results of the searches, and once these parameters are fixed, it is straightforward to estimate the exclusion provided by the LHC searches in terms of SMS. The interpretation of SUSY searches with SMS started back at the early LHC era, with the data collected at a centre-of-mass energy of 7 TeV. In [1], the CMS Collaboration summarised the main feature of the most common SMS used for the interpretation of the searches. The choice of such was driven by the sensitivity of the searches to the simple experimental signature provided by those SMS, and in particular it was stressed how the kinematics of the events was determined mainly by the mass scale of the SUSY particles involved, rather than other less important quantum or gauge numbers. While SMS prove useful to reduce the complexity of a full SUSY, or in general BSM theory, they require dedicated efforts to use such results to constrain arbitrary models that share similar kinematics properties. The main limitation concerns possibly complicated particle
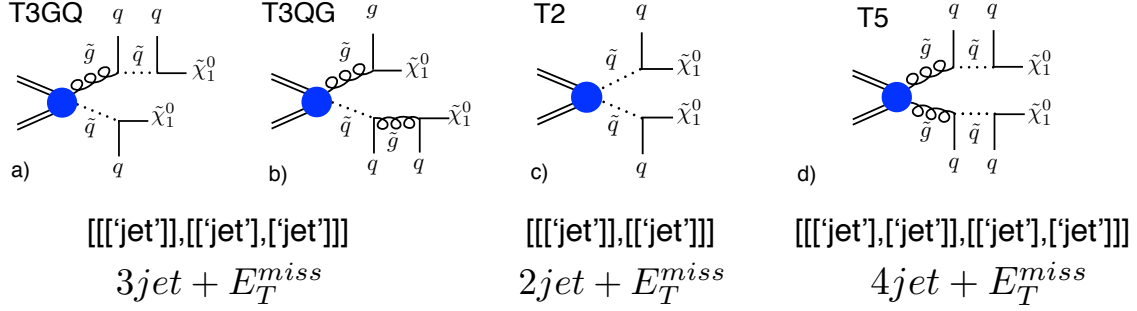
Figure 1: Diagrams for the simplified models used for the extension of the database. Models *T3GQ*(a) and *T3QG*(b), corresponding to the two different mass hierarchies $m_{\tilde{g}} > m_{\tilde{q}}$ and $m_{\tilde{q}} > m_{\tilde{g}}$, are identified by the experimental signature *[[['jet']],[['jet'],['jet']]]* in SModelS notation. Diagrams c) and d) represent the *T2* and *T5* models, mapping to the *[[['jet']],[['jet']]]* and *[[['jet'],['jet']],[['jet'],['jet']]]* signatures.

spectra and thus cascade decays to the lightest supersymmetric particles (LSP), whose kinematics might differ significantly from the simplified case. Moreover, by definition, the number of free parameters, i.e. of free particle masses in SMS should be kept small, and essentially the SMS commonly used for the interpretation of searches go up to three SUSY particles masses for cascade decays, or for asymmetric production (production of two different SUSY particles). For the task of re-interpretation of searches with SMS results, dedicated tools such as FastLim[2] and SModelS[3] were developed. They can decompose the signal of SUSY models into its SMS, and check the constraints provided by the LHC searches, contained in a dedicated database of results. In particular, SModelSwas used in [4] to study the coverage of the pMSSM-19[5] with SMS with respect to the full recast analyses performed by the ATLAS collaboration. Specifically, the set of pMSSM points considered were made public by the ATLAS collaboration on the HepData website[6]. The sensitivity of the ATLAS searches for a selection of BSM searches on the pMSSM was presented in [7]. They re-run their analyses on thousands of pMSSM model points, and characterized the constraints offered by each search considered for the reinterpretation .

The same model points were then tested with SModelS v1.1[8], obtaining a total coverage of roughly 55%-63% for the Bino and Higgsino-like LSP case, respectively. [1]. The work also showed that by means of efficiency maps (EM) results, that can be produced by phenomenologists outside the experimental collaborations, it was possible to increase significantly the number of ex-

cluded point. This is mainly due to the fact that the LHC collaborations provide results only for a limited set of SMS, and many interesting model, to which existing searches are sensitive to, are left unexplored.

Indeed, the comparison between the SModelS approach and the re-interpretation performed by the ATLAS collaboration showed that the main limitation of the simplified model approach is the lack of results for simple signatures, such as the $3jets$ + missing energy (E_T^{miss}). One of the SModelS tool main features is the ability of extracting the most relevant signatures in terms of $\sigma \times BR$ (production cross section times branching ratio) that are not currently constrained by simplified models results, called *missing topologies*. The aforementioned $3jets + E_T^{miss}$ signature can arise, for example, from gluino-squark associated production, where the gluino decays preferentially to an on-shell lighter squark, in turn decaying to a quark (that is reconstructed by the analysis as a jet of hadrons) and the LSP. This simplified model can be fully described by three mass parameters of the sparticle involved: $m_{\tilde{g}}, m_{\tilde{q}}$ and $m_{\tilde{\chi}_1^0}$. However, under the simplified model assumption, results for such model can be used to constrain the alternative mass hierarchy where the squark is heavier than the gluino, so that in this scenario the squark decays to on-shell gluino. The gluino can then decay radiatively to a gluon and the LSP or via an off-shell squark (i.e. 3-body decay, producing a $4jets + E_T^{miss}$ signature), depending on its mass difference with the lightest squark. The idea at the basis of this paper is to extend the previous study of the coverage of the pMSSM, and concretely show how the inclusion of newly created EM for the $3jets + E_T^{miss}$ signature increases the coverage of the pMSSM. This can be efficiently done by combining the information obtained with

---

[1]The Wino-like LSP dataset was neglected since most of the model pointed included long-lived charged particles, a signature which could not be handled by the v1.1 used.

SModelS regarding the important missing topologies, and the usage of analyses recasting tools to produce EMs results for arbitrary simplified models, to be implemented in the database of experimental results. For this purpose, this paper is structured as follows. Section 2 summarises the main characteristics of the $3jets + E_T^{miss}$ signature arising from gluino-squark production. In Section 4 the set up of the SModelSanalysis is described: the details regarding the production of the EMs for the gluino-squark model are discussed, and the set of pMSSM points used for the study are provided. Section 5 summarises the improved constrained obtained with the newly added EMs, in particular discussing the benefit of the signal combination from EM results. Finally an outlook about future extensions of the procedure is given in the conclusive Chapter 7.

2. The 3 jets + E_T^{miss} Signature

In generic pMSSM-19 points, the squark mass parameters are:

$$m_{\tilde{u}_L} = m_{\tilde{d}_L} = m_{\tilde{c}_L} = m_{\tilde{s}_L}$$

$$m_{\tilde{u}_R} = m_{\tilde{c}_R}$$

$$m_{\tilde{d}_R} = m_{\tilde{s}_R}$$

Since the mass of the gluinos is another free parameter, there are two possible mass hierarchies of interest. When considering for simplicity the lightest of the squark masses with $m_{\tilde{g}} > min(m_{\tilde{q}})$ (and the other third generation squark set to a high scale), gluino will decay almost entirely to an on-shell intermediate squark, followed by the decay of the squark to the LSP:

$$pp \to \tilde{g}\tilde{q}, \tilde{g} \to \tilde{q}q, \tilde{q} \to q\tilde{\chi}_1^0 \qquad (1)$$

However, for the alternative hierarchy where the squark considered is heavier than the gluino, $min(m_{\tilde{q}}) > m_{\tilde{g}}$ the squarks will decay to an on-shell intermediate gluino. The gluino will then decay either via radiative decay to the LSP as

$$pp \to \tilde{g}\tilde{q}, \tilde{q} \to \tilde{g}q, \tilde{g} \to g\chi_1^0 \qquad (2)$$

or, for small $\Delta M(min(m_{\tilde{q}}), m_{\tilde{g}})$, via a three-body decay from off-shell squark:

$$pp \to \tilde{g}\tilde{q}, \tilde{q} \to \tilde{g}q, \tilde{g} \to q\bar{q}\tilde{\chi}_1^0. \qquad (3)$$

The simplified model of interest of this work produces a $3jet +$ missing energy final state as formulated in the Decays 1 and **??** [2] This experimental signature, also called constraint, can be obtained by considering two different mass hierarchies, which are depicted by the diagrams a) and b) in Fig. 1. The first, labelled T3GQ represents the case where the gluinos are heavier than the squarks considered; the latter, labelled T3QG represents the alternative case. Note that for our purposes, it is sufficient to consider only the lightest of the three squarks. Depending on the specific pMSSM model point considered, one of the two alternative mass hierarchies will produce this specific signature, due to the strong nature of the gluino-squark coupling. As stated in the introduction, the T3GQ model was found to be the most important missing result for the pMSSM. It is to note, however that, by construction, the T2 and T5 models, represented by plots c) and d) of Fig. 1, are automatically important when the T3GQ model also is. In practice, the T3GQ model is an asymmetric model composed by one branch from the T2 and one branch from the T5 models. Thanks to the usage of EM results, it is thus possible to combine the signals from the $pp \to \tilde{g}\tilde{g}$, $pp \to \tilde{q}\tilde{q}$ and $pp \to \tilde{g}\tilde{q}$ channels. Along with the results from TGQ, the power of combining the T2 and T5 models will be explored in this work. For completeness, results for the T2 and T5 models were already included in the previous release of the database, hence did not appear in the missing topologies list of the original study.

3. Production of the Efficiency Maps

The set-up for the production of the Monte Carlo signals is the following. Events at parton level were generated using MadGraph5_aMC@NLO[9], and then showered and hadronized using Pythia 6.4[10]. The processes considered for the production of the samples for the simplified model are described in Tab. 1. Note that the processes considered the emission of up to one extra parton. The syntax $go Q is used to avoid the presence of on-shell resonances, represented by intermediate gluino or squarks, that would lead to double counting when performing the merging between matrix-element and parton-shower. The merging between the matrix elements and parton-shower formalisms was performed adopting the k_T jet MLM scheme [11, 12]. The analysis recasting

---

[2]Both correspond to the *[[['jet']],[[['jet'],['jet']]]* signature in the SModelS language.

MadGraph5_aMC@NLO processes
T2: $pp \to \tilde{q}\tilde{q}$
define Q = dl dr dl˜dr˜ul ur ul ˜ur˜
generate p p > Q Q
add process p p > Q Q j
T5: $pp \to \tilde{g}\tilde{g}$
generate p p > go go
add process p p > go go j
T3GQ: $pp \to \tilde{g}\tilde{q}$
define Q = dl dr dl˜dr˜ul ur ul˜ur˜
generate p p > go Q \$ go Q
add process p p > go Q j \$ go Q

Table 1: MadGraph5_aMC@NLO processes for the production of the Monte Carlo samples.

was performed with MadAnalysis 5, using the recasting codes for the analysis ATLAS-SUSY-2013-02[13, 14] and CMS-SUS-13-012[15, 16]. The tuned version of DELPHES 3 integrated in the MadAnalysis 5 framework was used to take into consideration the detector efficiency on the particles. Jets were clustered using FastJet[17]. The description of the grid of mass points defined for the production of the efficiency maps is provided in Tab. 2. The analyses chosen for the recasting search for SUSY events in the all hadronic final state, vetoing the presence of isolated leptons. In particular the two above analyses are sensitive to events with small jet multiplicity, as generated by the simplified models considered. Although official EM results for the *T2* model were made public by the collaborations, part of the parameter space with small mass gap between the squark and the LSP is below 50 GeV is not properly covered. For this reason, EMs were produced to replace the official results, up to a mass difference as small as 5 GeV between the squarks and the LSP. In addition, also the results for the *T5* model were extended to cover scenarios with small mass difference between the gluino-squark and squark-neutralino The parameter x is defined so that

$$m_{\tilde{q}} = x \cdot m_{\tilde{g}} + (1 - x) \cdot m_{\tilde{\chi}_1^0}. \qquad (4)$$

For the *T3GQ* model, the gluino mass reaches the value of 2 TeV, with a binning of 50 GeV for $200 \leq m_{\tilde{g}} < 1200$, and a binning of 100 GeV for $1200 \leq m_{\tilde{g}} \leq 2000$ GeV. The squark masses for the *T3GQ* have a 50 GeV binning, and reach the maximum value of 1 TeV. For a better coverage

of the parameter space in the case of small mass differences, additional mass planes parametrized with

$$\Delta M(\tilde{q}, \tilde{\chi}_1^0) = (5, 10, 15) \; GeV \qquad (5)$$

were produced. Note that the values of the maximum values of the gluinos and squarks were chosen arbitrarily, since a priory there is no possibility to determine the efficiency of the analysis and of the cross section upper limit. It will be see in Section **??** that indeed this limit should be extended to regions of larger $m_{\tilde{g}}$, since both the efficiency of the recast analyses considered and the associated gluino-squark production cross sections are sufficiently sizeable The mass hierarchy used

Mass Planes	
T2: $pp \to \tilde{q}\tilde{q}$	
-	$\min(\Delta M(\tilde{q}, \tilde{\chi}_1^0)) = 5$ GeV
T5: $pp \to \tilde{g}\tilde{g}$	
x=(0.05,0.50,0.95)	
$\Delta M(\tilde{q}, \tilde{\chi}_1^0) = 5$ GeV	
T3GQ: $pp \to \tilde{g}\tilde{q}$	
$m_{\tilde{g}} = 200,...,1200$	50 GeV bin
$m_{\tilde{g}} = 1300,...,2000$	100 GeV bin ($m_{\tilde{g}} \leq 2$ TeV)
$m_{\tilde{q}}$	50 GeV bins ($m_{\tilde{q}} \leq 1$ TeV)
	$\min(\Delta M(\tilde{q}, \tilde{\chi}_1^0)) = 5$ GeV

Table 2: Mass plane parametrization used for the EMs production of the *T2*, *T3GQ* and *T5*. See the text for details.

for the production of the gluino-squark model is $m_{\tilde{g}} > m_{\tilde{q}}$, meaning that the *T3GQ* model was chosen to constrain the "[[['jet']],[['jet'],['jet']]]" signature. Note that the same problem related to the choice of the mass hierarchy applies to the *T5* model: the "[[['jet']],[['jet']]]" signature can be obtained both with $\tilde{g} \to g\tilde{\chi}_1^0$ and $\tilde{q} \to q\tilde{\chi}_1^0$. Also for the recasting of this model the former hierarchy was chosen. In Appendix Appendix A the comparison between the values of the upper limits and efficiencies obtained for the two different mass hierarchy, for two benchmark points, are provided. Differences can indeed arise due to the different hadronization and clustering of quarks and gluon into jets, so that the jets momentum and multiplicity, and linked kinematics variables such as the hadronic transverse energy, might differ. However such differences have a limited impact in the efficiency selection, typically contained within 20%. The observed UL calculation, however, is based on the selection of best expected signal region, i.e. the signal region which provides the best expected limit. The observed num-

ber of events indeed suffer from statistical fluctuation, that might be quite different from one signal region to another. For this reason, a small difference in the efficiency might lead to the selection of a different signal regions providing the best expected limit, and consequently to a discording observed UL from SR to SR. While this might result in up to a factor 2 difference in the observed UL, this translates into a modest uncertainty in the cross section UL and in the mass of the related SUSY particle, with little impact in the general interpretation of the excluded regions of the parameter space of the tested pMSSM-19. It is important to stress that `SModelS` does not distinguish between gluon and light quarks in the final states, both generically identified as "jet". This happens with the *T3GQ* model as seen explicitly in Fig. 1 a) and b) diagrams, where both quark and gluon jets appear. Consequently also also the *T2* and *T5* results can be used to constrain the alternative models $pp \to \tilde{g}\tilde{g}, \tilde{g} \to \tilde{g}\chi_1^0$ and $pp \to \tilde{q}\tilde{q}, \tilde{q} \to \tilde{g}q, \tilde{g} \to g\tilde{\chi}_1^0$.

4. Simplified Model Analysis Setup

We describe in this Section the setup at the basis of our analysis of the pMSSM: we introduce the basic features of the `SModelS`tool, we describe the experimental results considered and then selection of the pMSSM-19 points.

4.1. SModelS Workflow

To explore the constraining power of the plenty of SMS results produced both by the LHC collaboration and by groups of phenomenologists, the tool `SModelS`[8, 18, 19] offers an efficient interface between the theory predictions for arbitrary BSM models and the experimental data. While up to version 1.1 the BSM models were assumed to satisfy a $\mathcal{Z}_\in$ symmetry resulting in a missing energy signature in the detectors, the most recent version extends its capabilities to long lived charge particles. However, these are not the interest of this work, where it is assumed that each SMS has a pair production of SUSY particles forming two branches, each of them terminating with a χ_1^0 as LSP responsible of the missing energy signature. The two main steps at the basis of the `SModelS`workflow are the decomposition od the input BSM model into a spectrum of simplified models, and the comparison of the theory prediction associated with each simplified model to the experimental cross section UL. The UL can be provided directly by the LHC collaborations, under the form of UL maps, or they can be calculated using a the simplified CLs prescription (see

e.g. [20, 21]) starting from the analyses efficiency, for each separate signal region, and the experimental information of the number of expected background events n_{exp}, its related uncertainty Δn_{exp} and the number of observed events n_{obs}. UL maps cannot be used to combine signals for different SMS, and can be used only individually. Thanks to signal combination, efficiency maps results often offer stronger limits; however, it is not possible to exploit the full power of signal regions (SRs) combination, either because they are overlapping and events might fall in more than one SR, or because of lack of the correlation matrices, not available for the LHC Run 1 results. This forces to consider only separate SRs, and the limit considered is the one provided by the "best" SR, defined as the SR giving the strongest expected limit (setting $n_{obs} \equiv n_{exp}$). This is done to avoid biases in the SR selection due to statistical fluctuations in the experimental data; finally, the observed UL of the best SR is calculated. The parameter $r\ value$:

$$r\ value = \frac{\sigma_{Theo}}{\sigma_{UL}} \quad (6)$$

is then extracted for each result. The quantity σ_{Theo} corresponds to the weight $\sigma \times BR$ of each simplified model in the decomposition for UL results, or sum of weights for EMs results. A model point is excluded if, for at least one experimental result, the corresponding theory prediction exceeds the value of the UL. `SModelS` does not perform any statistical treatment of the $r\ value$.

4.2. Selection of the pMSSM-19 Model Points

The setup for the analysis with `SModelS` follows closely what described originally in [4], that is here summarized. The pMSSM-19 model points considered represent a subset of the dataset originally used by the ATLAS collaboration in the re-intepretation study[7], and made available on `HepData`[6] in the form of SLHA[22] files. The details regarding the production of the model points and the selection criteria can be found in the original phenomenological papers [23–26]. They split the regions of the parameter space according to the nature of the LSP, represented in this model by the lightest of the four neutralinos, divided into Bino, Higgsino and Wino-like nature, as:

- **Bino-like LSP** for $N_{11}^2 > max(N_{12}^2, N_{13}^2 + N_{14}^2)$ [103,410];

- **Wino-like LSP** for $N_{12}^2 > max(N_{11}^2, N_{13}^2 + N_{14}^2)$ [80,233];

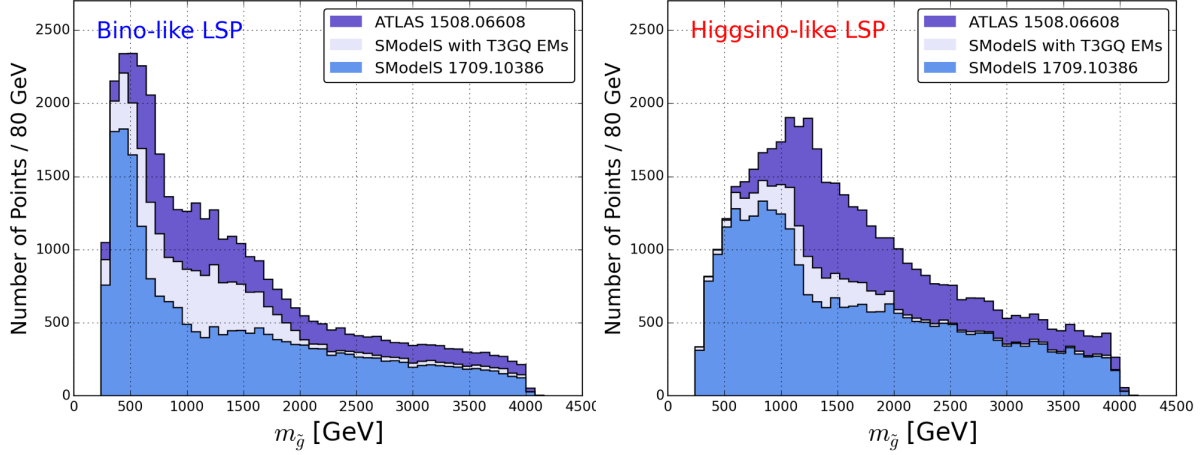- **Higgsino-like LSP** for $(N_{13}^2 + N_{14}^2) > max(N_{11}^2, N_{12}^2)$ [126,684,

Figure 2: Distributions of the points excluded by ATLAS (purple), by SModelS with the inclusion of the newly homegrown maps (light blue), and by the previous work [4] (slate blue), for the Bino(top) and Higgsino-like LSP (bottom).

where N_{ij} are the entries in the neutralino mixing matrix (see e.g. [27]). In square brackets, the total numbers of parameters points tested in the AT-LAS study is reported. for these more than 300k model points, the ATLAS collaboration produced Monte Carlo samples and re-run a selection of Run 1 searches for BSM physics. The SModelS coverage study investigated only the subset of points which could at least be excluded by at least one canonical SUSY search based on missing energy signature. Justified by the main purpose of quantifying the coverage of the pMSSM by means of simplified model results, the model points that could be excluded only by searches for resonant heavy Higgs bosons, or by searches for exotic charged particle that give origin to signatures such as displaced vertices, were not considered, since SMS results for such searches do not exists. This requirements reduced the original number of points tested by ATLAS from 103,410 to 38,575 (Bino-like LSP dataset) and from 126,684 to 45,594 (Higgsino-like LSP dataset). These surviving points were passed through SModelS and analyzed, and constitute the same dataset for the new analysis presented in this work, aiming at showing the improvement in the coverage thanks to the newly added efficiency maps results.

The same version v1.1.1 of SModelS was employed. The SModelS cross section calculator, which provides a useful interface with Pythia 8(v.8.226)[28], Pythia 6[10] and NLLFast [29–36] was used to compute the production cross sections, up to NLO+NLL order for strong production, and LO for electroweak processes; Pythia 6 was instead used for slepton production. The other two relevant parameters selected in the configuration file parameters.ini are the

sigmacut= 0.03 fb, that controls the minimum allowed weight $w = \sigma \times BR$ for each simplified model appearing in the decomposition, and minmassgap = 5 GeV, i.e. the minimum mass gap for which the SM products appearing in the decay chain are considered visible.

4.3. SModelS Database

We used the complete set of SMS results available for 8 TeV centre-of-mass energy of the release 1.1.1 of the database. These include official results in the form of upper limits and efficiency maps from the ATLAS and CMS collaborations, EMs results produced by the FastLim collaboration available at [37] and adapted to the SModelS infrastructure, and the set of EM results recast by SModelS collaboration. The complete description of the database of v1.1.1 can be consulted in [4]). In addition we added the EM results specifically produced for this work described in Section 3. Concretely, the additional EMs results in the updated database are:

- ATLAS-SUSY-2013-02: *T2* (which replaces the maps officially provided by ATLAS), *T5* and *T3GQ* results;

- CMS-SUS-13-012 *T2* (which replaces the maps officially provided by CMS) and *T3GQ* results.

The replacement of the *T2* results was done in order to cover smaller mass gaps, as described in Tab. 2. The new EMs were made available with the database release 1.2.2. All the versions of SModelS databases can be consulted at [38]. For convenience, all the EMs results that will discussed when presenting the extension of
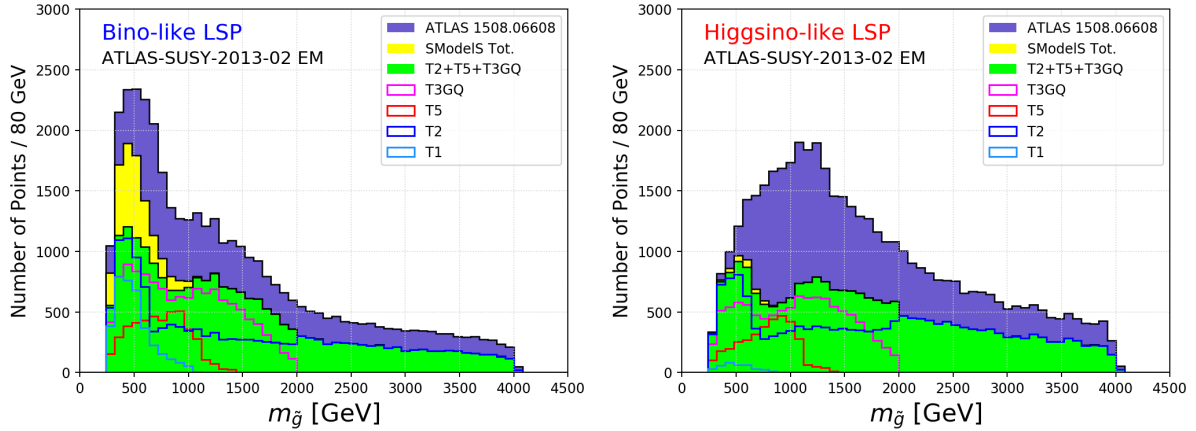
Figure 3: Contribution of the *T1*, *T2*, *T5* and *T3GQ* simplified model results and their combination for the analysis ATLAS-SUSY-2013-02, as a function of $m_{\tilde{g}}$.

the pMSSM-19 coverage are summarised in Tab.3. Note that several EMs results were recast for the CMS-SUS-13-012 analysis, and already employed for the coverage in the first study.

ATLAS-SUSY-2013-02 , CMS-SUS-13-012		
SMS	Decay	Source
T1	$pp \to \tilde{g}\tilde{g}, \tilde{g} \to q\bar{q}\tilde{\chi}_1^0$	Official
T2	$pp \to \tilde{q}\tilde{q}, \tilde{q} \to q\tilde{\chi}_1^0$	Recast
T5	$pp \to \tilde{g}\tilde{g}, \tilde{g} \to \tilde{q}q, \tilde{q} \to q\tilde{\chi}_1^0$	Recast
T3GQ	$pp \to \tilde{g}\tilde{q}, \tilde{g} \to \tilde{q}q, \tilde{q} \to q\tilde{\chi}_1^0$	Recast

Table 3: Summary of the EMs considered in the extension of the pMSSM-19 coverage.

5. Extending the pMSSM Coverage

In this Section we study the improvements in the pMSSM coverage provided by the additional EMs for the *T3GQ* gluino-squark model, in combination with the *T2* and *T5* model.

Table 4 shows the new total exclusion of the pMSSM points, 21,151 and 28,669 points for the Bino and Higgsino-like case, allowing to cover the 74 and 71 % of the total points tested. With respect to the previous coverage detailed in [4], an improvement in the coverage of +19% and +8% respectively is obtained. The major improvement appears in the Bino-like LSP case, as noticeable also in the gluino and squark mass coverage distributions in Fig. 2. Due to the choice of the parametrisation of the mass planes for the sample

	ATLAS	SModelS(EM+UL)
Bino LSP		
	38527	28765 (74 %)
Higgsino LSP		
	45345	32358 (71 %)

Table 4: SModelS constraints for the Bino and Higgsino-like LSP after the addition of the newly implemented EMs results for the models *T2*, *T5* and *T3GQ*.

production, the bulk of the improvement is found for $m_{\tilde{g}} \leq 2$ TeV. The extension of the EM to cover of the small mass gaps between the squarks and the LSP, as described in Tab. 2, gives important contribution to the exclusion not only for large gluino masses, but also for intermediate to low mass values. This can be understood by looking at Fig. **??**, that reports in colour code the total SModelS r value for the Bino-like LSP dataset, focussing on the points that could not be excluded with the previous version of the database. Since the results for the Higgsino-like dataset show similar characteristics, they are not here reported. The results are projected on the $(m_{\tilde{g}}, min(m_{\tilde{q}}))$ mass plane. As a general consideration it can be noticed that many points exhibit a large *r value*, exceeding the limit *r vale* > 10 in red colour. While it considered sufficient that *r value* > 1 for a model point to be considered excluded, the analysis of the distribution of the *r value* can be used for a quantitative yet crude estimation of the uncertainties of the SModelS procedure and of the uncertainties on the theory level; this will be later discussed in Section 5.2.

7

5.1. Breakdown of the SMS Results

As detailed in Section 2, the *T2*, *T5* and *T3GQ* can be combined to reconstruct more comprehensively the signals from $\tilde{g}\tilde{g}$, $\tilde{q}\tilde{q}$ and $\tilde{g}\tilde{q}$ production channels. Here we wish to analyse how the newly excluded points benefit from such combination. We limit ourselves to consider only the analysis ATLAS-SUSY-2013-02, since similar conclusions can be obtained for the CMS-SUS-13-012 analysis. In addition we to the recast results, EMs for the *T1* model

$$pp \to \tilde{g}\tilde{g}, \tilde{g} \to q\bar{q}\tilde{\chi}_1^0 \ , \tag{7}$$

i.e. gluino decay to the LSP via off-shell light squarks, provided by the ATLAS collaboration, are used. The exclusions from each model and from the combination of the $T2 + T5 + T3GQ$ are drawn in Fig. 3. Note that points can be excluded by more than one results, e.g. points with both light squarks and gluinos, with $m_{\tilde{g}} > m_{\tilde{q}}$, might be excluded by both the *T2* and *T5* results; for this reason, the histogram relative to each SMS cannot be stacked together. A major difference between the Bino and the Higgsino-like LSP case concerns the exclusion from the *T1* results, which are significant in the former case, but almost irrelevant in the latter. The model is considered for completeness since such result is available. However, this signal cannot be in general combined with the other signatures of interest, since the *T1* model arises most frequently from the decay of a gluino decaying to an off-shell squark, which is by construction a competing decay channel with respect to the *T3GQ* model.
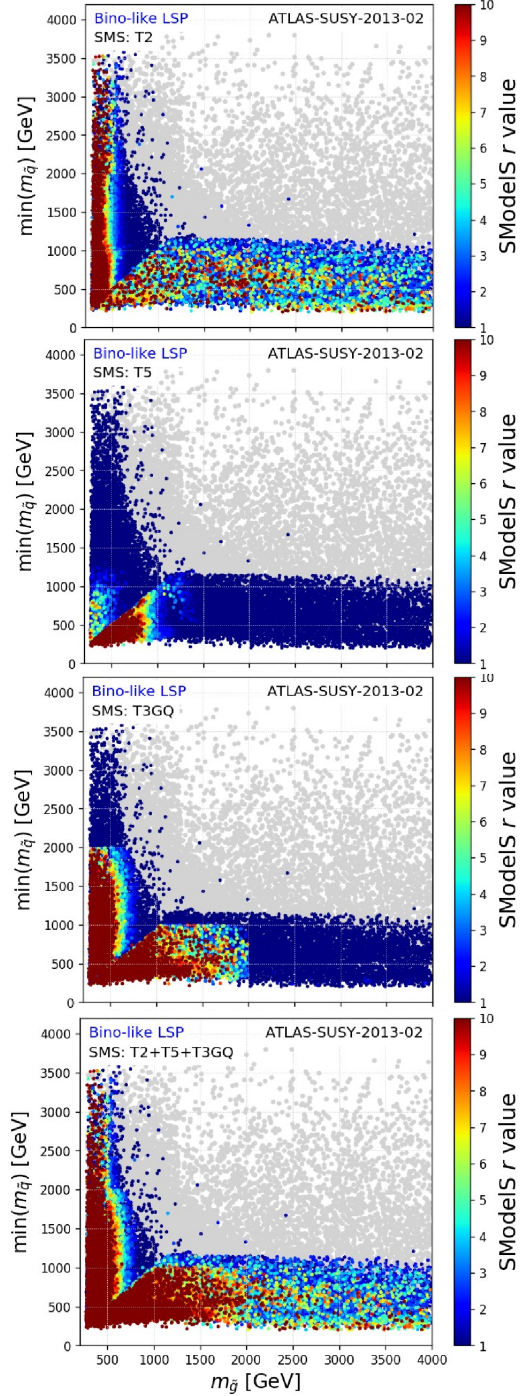
Other SUSY configuration can still result in the *T1* signature, for example the production of charginos and neutralinos decaying hadronically to off-shell vector bosons, but they are practically irrelevant due to the small $\sigma \times BR$. In Fig. A.10 the contribution of the model carrying the largest r value (or partial weight) among the available *T1*, *T2*, *T5* and *T3GQ* is highlighted. For the majority of the points, this values amount to around half of the total weight, calculated using all the available EM results. Besides taking advantage of the availability of recasting tools, EM results are also extremely useful since they allow for the combination of signals, allowing for the reconstruction of full SUSY events.

In the case of the *T2*, *T5* and *T3GQ*, the squark-squark, gluino-gluino and gluino-squark productions and their consequent decays to the LSP. Finally, in Fig.**??**, the distributions of the r values for each result of the analysis ATLAS-SUSY-2013-02 (*T1,T2,T5* and *T3GQ*), the combinations of models (*T2+T5*, *T2+T5+T3GQ* and the sum of all the available results *T1+T2+T5+T3GQ*) is show. Only the points excluded by the analysis are considered; this implies that the points in the first bin $0 \leq r < 1$ can be excluded only by considering the sum of all the results, i.e. considering *T1+T2+T5+T3GQ*. For the bins with $r \geq 1$, each individual contribution might be sufficient to exclude the models tested. For large rvalues, the number of points decreases as expected, and the importance of the combinations of multiple results increases. The last bin refers to $rvalue \geq 10$, i.e. points that can be strongly excluded by the SMS results considered, in particular by the combination of the *T1+T2+T5+T3GQ* and *T2+T5+T3GQ* for the Bino and Higgsino-like LSP case respectively. As stressed when introducing EMs, one of the advantages of using such kind of results is the possibility to combine the different SUSY signals that map onto the decomposed SMS. In Table 5 Finally, in Figures

Figure 4: Distributions of the r *value* for *T2*, *T5*, *T3GQ* and their combination for the points excluded by the ATLAS-SUSY-2013-02 results (Bino-like LSP dataset). Grey points have a total r value ≤ 1. A large portion of points excluded bz *T2* lies in the $m_{\tilde{g}} < 500$GeV mass, due to the gluino loop decay $\tilde{g} \to g\tilde{\chi}_1^0$. A similar argument holds for the *T5* model, in the region where the result constrains the $\tilde{q} \to q\tilde{g}, \tilde{g} \to g\tilde{\chi}_1^0$ decay. The *T3GQ* model results can efficiently constrain the two alternative mass hierarchies $m_{\tilde{g}} > m_{min(\tilde{q})}$ or $m_{min(\tilde{q})} > m_{\tilde{g}}$. In particular it shows that the EMs should be extended to cover $m_{\tilde{g}}$ masses larger than the 2 TeV values.

SMS	Bino	Higgsino
T1 : $pp \to \tilde{g}\tilde{g}, \tilde{g} \to q\bar{q}\tilde{\chi}_1^0$	3174	204
T2 : $pp \to \tilde{q}\tilde{q}, \tilde{q} \to q\tilde{\chi}_1^0$	7221	11180
T5 : $pp \to \tilde{g}\tilde{g}, \tilde{g} \to q\tilde{q}, \tilde{q} \to q\chi_1^0$	191	160
T3GQ : $pp \to \tilde{q}\tilde{g}, \tilde{g} \to q\tilde{q}, \tilde{q} \to q\chi_1^0$	3259	2792
T2 + *T5* + *T3GQ*	3320	299

Table 5: Number of points that can be excluded only by including each individual result for *T1*, *T2*, *T5*, *T3GQ*, or their combination. See the text for details.
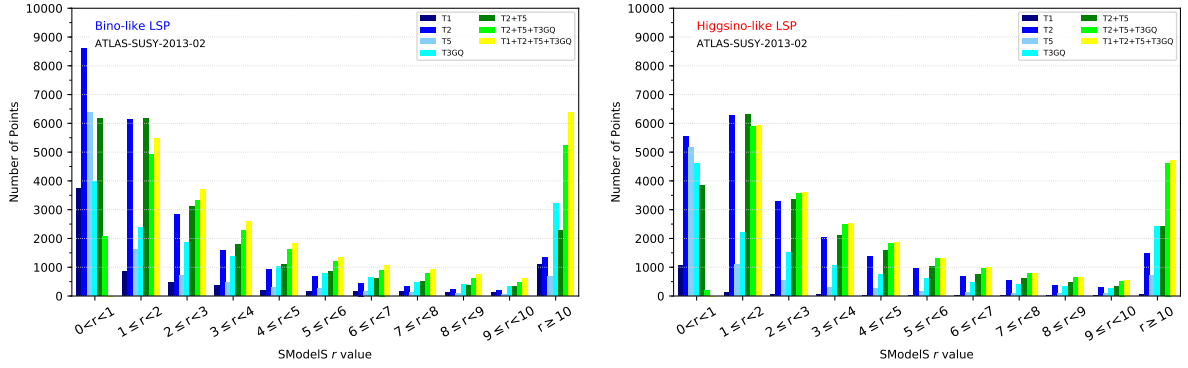
Figure 5: Distribution of the r values for excluded points, considering single SMS or combinations, for the analysis ATLAS-SUSY-2013-02. The points included in the first bin $0 < r\ value < 1$ can only be excluded by the combination of all the EMs results available for the ATLAS-SUSY-2013-02 analysis.

4 and **??** the distribution for the r-values for the $T2$, $T5$, $T3GQ$ models and their combination is shown, for the Bino and Higgsino-like LSP cases respectively. The contribution from the $T1$ model, for which results exist, are not considered. Note that the plots are projected onto the $(m_{\tilde{g}}, min(m_{\tilde{q}}))$ mass plane. This highlights the contribution from the two alternative mass hierarchies $m_{\tilde{g}} > min(m_{\tilde{q}})$ or $min(m_{\tilde{q}}) > m_{\tilde{g}}$, clearly indicated by the points distributed around the diagonal of the plots.

5.2. Estimation of the Uncertainties

In this section we provide a rough yet qualitative estimation of the uncertainties of the whole procedure. These are very challenging to estimate reliably due to the complexity of the procedure itself, which involves at first the production of the Monte Carlo events for the generation of the event files, then the analyses recast. The validation documents provided with the analyses recasting code is a valid proof that the choice of the simulation parameters allows to reproduce well the analyses efficiency. While the generation of a sufficient amount of events keeps the statistics uncertainty under reasonable control, systematic effects are not taken into accounts. Last but not least, the entire assumptions at the basis of the simplified model spectra idea inevitably introduces approximations, due to neglecting the production mechanisms of the SUSY particles considered (since the events are produced with decoupled spectra) and any kinematics effects due to the quantum numbers of the particles. All these aspects add up together and cannot be easily quantified. As formulated in the definition of `SModelS` $r\ value$ in Eq. 6, a model point is considered excluded if the

$r\ value$ exceeds unity. Tightening this condition by requiring that the theory predictions exceeds higher value can mimic the inclusion of uncertainties on the theory level (e.g. on the reference cross section calculation, on the recasting procedure and/or on the SMS assumptions). In Fig. 6 the distribution of the excluded points, as a function of $m_{\tilde{g}}$, is plotted for different $r\ value$ requirements of $r\ value > 1$ (standard exclusion criterion used throughout the paper), and $r\ value > 1.2, 1.5, 2.0$, corresponding to a decrease in the theory predictions of $20\%, 50\%, 100\%$. These higher values result in more conservative exclusion. The total number of points excluded considering each separated value is reported in the legend. It is comforting to note that even for the pessimistic case of the largest uncertainty, the number of points does not differ for more than 25% with respect to the standard criterion. There is also no sign of higher impact which depends on $m_{\tilde{g}}$, so any systematic effect dependent on this mass parameter should be improbable. We finally note than a similar methodology was employed by the AT-LAS collaboration to determine the exclusion of the model points. In particular, the uncertainty on the theory cross section calculation was estimated up to 100%, but unfortunately such values are not available.

6. A Look at 13 TeV Results

In this Section we discuss briefly what happens with SMS results produced with 13 TeV centre-of-mass energy collision data. Due to the large increase in the production cross section, it is expected that the coverage of the pMSSM-19 for the same dataset of points designed for 8 TeV results, increases considerably. In fact, this was already
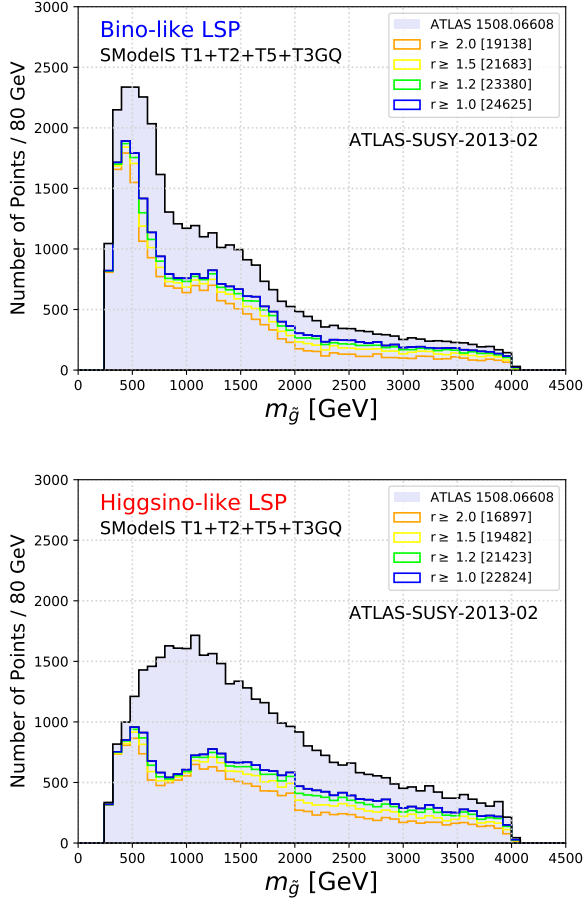
Figure 6: Distribution of the excluded points, as a function of $m_{\tilde{g}}$, for different requirements of $r \ value >$ $1.0, 1.2, 1.5, 2.0$. Only the EM results for the analysis ATLAS-SUSY-2013-03 are used, for the SMS T1 (official results form ATLAS) and $T2$, $T5$, $T3GQ$ (homegrown `SModelS` results). On top, the total number of points excluded by the official ATLAS study only the aforementioned analysis is shown.

Figure 7: Distribution of points (Bino-like LSP dataset) excluded by the 8 TeV EM results for the analysis ATLAS-SUSY-2013-02, but not excluded by recent 13 TeV analyses published in v1.2.2 of the `SModelS` database. In cyan, the points fall outside the grid of results available for 13 TeV results; in purple, points for which the 13 TeV $r \ value < 1$. Note that most of the points lies in the region of small gluino/squark-LSP mass gap.
.

shown in [40]: by using SMS results for a selection of 13 TeV analyses, with collision data adding up to around 36 fb^{-1}, almost all the entire set of pMSSM-19 points considered by ATLAS could be excluded, including points out of reach with 8 TeV searches. The aim of the present discussion is to demonstrate that, despite the large increase in the production cross section, certain regions of the parameter space cannot be covered even with the latest results. In Fig. 7 we consider a set of points which can be excluded with the new ATLAS-SUSY-2013-02 EMs, but cannot be excluded by the 13 TeV results implemented in the most updated release v.1.2. of the `SModelS` database. The points are divided into two categories. The first include points that do not map onto any of the available results, mainly because the mass array characterising the models in the decomposition

cannot be mapped onto the mass grid of the results. The second category includes points for which 13 TeV results can indeed be applied, but they prove insufficient to exclude the points. The two different mass planes show clearly that indeed the majority of points falls in the region where the mass gap between the gluino-LSP or squark-LSP is small. In Fig. 9 we also include the distributions of 8 TeV ATLAS-SUSY-2013-02 results, which reaches up to values greater than few tens.

We note that the recent Run 2 inclusive ATLAS 0 lepton,2-6 jets search[?], that uses 36 fb^{-1} of collision data, is interpreted with gluino and squark pair production and gluino-squark SMS. In particular, the gluino-squark model is in fact a realisation of the pMSSM where only 1st and 2nd generation squarks and gluinos are consid-

Figure 9: Mass spectrum of the point 457584173, from the Bino-like LSP dataset.

.

Figure 8: Distribution of points (Bino-like LSP dataset) excluded by the 8 TeV EM results for the analysis ATLAS-SUSY-2013-02, but not excluded by recent 13 TeV analyses published in v1.2.2 of the `SModelS` database. In cyan, the points fall outside the grid of results available for 13 TeV results; in purple, points for which the 13 TeV $r\ value < 1$. Note that most of the points lies in the region of small gluino/squark-LSP mass gap.
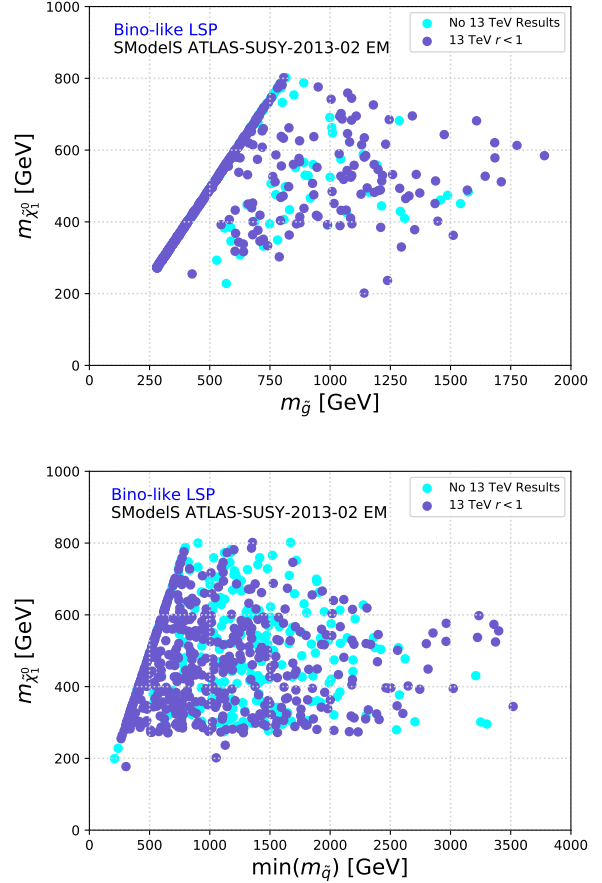
.

ered, and all the other sparticles are decoupled. They parametrized the mass planes by fixing the LSP mass (Bino-like, for $m_{\tilde{\chi}_1^0} = (0, 695, 995)$ and considered a grid of gluino and squark masses. We note that the in order to use such results, an interpolation in the LSP mass of around 700 GeV, to cover the region $m_{\tilde{\chi}_1^0} < 700$ GeV , has to be performed. Unfortunately the results are provided (on `InspireHEP`[?] only in the form of UL maps. It would be much appreciated if EMs for the gluino-squark model were also made available and allow for the combination with the published EMs for the *T2* model. Finally, we provide the results of one of such points, the SLHA file 457584173 from the Bino-like LSP dataset. The mass spectrum, obtained with `pySLHA`, is shown in Fig. **??**.

7. Conclusion

While simplified models have become hugely popular among the experimental collaboration for the interpretation of their BSM searches, it is always challenging to make use of such results to investigate complicated theories. Moreover, the question if the simplified approach is sufficient to properly cover the a full model is always open. A big step forward, for the case of the pMSSM-19, was taken in [?] , where it was shown that a large portion of the parameter space of such SUSY model can be efficiently constrained by means of SMS, without the computationally

expensive procedure of analyses recasting. At the same time, despite the plenty SMS results, there is a lot of room for improvement in the coverage. Certainly, the very essence of SMS makes them inadequate in the presence of complicated mass spectra, that give rise to long decay patterns and that are better captured by full analyses recast. Fortunately the main outcome of the previous study showed clearly that for the majority of uncovered model points, most of the unconstrained $\sigma \times BR$ was captured by a class of simplified models involving only three SUSY particles and short decay, arising from gluino-squark production. The associated $3jets + MET$ signature is easily covered by inclusive all hadronic final state searches at the LHC, targeting specifically low jet multiplicity, such as ATLAS-SUSY-2013-02 and CMS-SUS-13-012. The results presented in this work show concretely that it is possible to produce such dedicated EM results, using available recastign tools, and significantly increase the coverage of the model up to 74Moreover, due to the large cross section for gluino-squark production, it was shown that the new EMs could be still extended to larger particle mass, and obtain additional constraints. The workflow can be extended and implemented for other theories: once the most important missing simplified signatures are determined, recast EM can be produced only once, and the results can be re-used to constrain generic models. In addition to the possibility to produce customized SMS results, EMs have the advantage of allowing the combination of multiple signals. In particular, the combination of the *T2+ T5+ T3GQ* signals for the ATLAS-SUSY-2013-02 analysis is sufficient to cover the XX and XX of the points covered by the full recast of the analysis, as performed by ATLAS. We note that this is obtained by neglecting most of the

popular simplified model for gluino production, such as the direct decays of gluinos via off-shell top $pp \to \tilde{g}\tilde{g}, \tilde{g} \to t\bar{t}\chi_1^0$ and sbottom squarks $pp \to \tilde{g}\tilde{g}, \tilde{g} \to b\bar{b}\chi_1^0$, and models for third generation squarks direct decay such as $pp \to \tilde{b}\tilde{b}, \tilde{b} \to b\chi_1^0$ and $pp \to \tilde{b}\tilde{b}, \tilde{b} \to b\chi_1^0$, to which the search is expected to be sensitive to (see e.g. [39] for the top squark model). On another note, we are aware that the latest data, referring to proton collisions at 13 TeV centre-of-mass energy, give much better constraints on the same model due to the significant increase in the production cross section, and also in the larger amount of data, since the latest SUSY searches form the ATLAS and CMS collaborations are based on an integrated luminosity of around 140 fb^{-1}, already a factor 7 higher than the luminosity collected during Run 1. The impact on the pMSSM-19 was already estimated in [40]. There is however a substantial difference and outcome in the aim of the two works. With this study, we aimed at somehow give a concrete exemplification of systematic use of the tool SModelS in association with public recasting tool to improve what is the state of the art of the available SMS results. Stressing the importance of specific simplified models results, produced for specific SUSY searches, is valuable information for the future. In fact, still neither the $T5$ nor the $T3GQ$ models are available at higher centre-of-mass energy, being those official or recast results. This works constitute a solid starting point for building future updates of the databases of SUSY SMS results, and we invite both the experimental collaboration and our colleague phenomenologists to produce UL and/or EM results for the SMS here studied.

Acknowledgments

References

[1] **CMS** Collaboration, S. Chatrchyan et al., *Interpretation of Searches for Supersymmetry with simplified Models*, *Phys. Rev.* **D88** (2013), no. 5 052017, [arXiv:1301.2175].

[2] M. Papucci, K. Sakurai, A. Weiler, and L. Zeune, *Fastlim: a fast LHC limit calculator*, *Eur. Phys. J.* **C74** (2014), no. 11 3163, [arXiv:1402.0492].

[3] S. Kraml, S. Kulkarni, U. Laa, A. Lessa, V. Magerl, W. Magerl, D. Proschofsky-Spindler, M. Traub, and W. Waltenberger, *SModelS v1.0: a short user guide*, arXiv:1412.1745.

[4] F. Ambrogi, S. Kraml, S. Kulkarni, U. Laa, A. Lessa, and W. Waltenberger, *On the coverage of the pMSSM by simplified model results*, *Eur. Phys. J.* **C78** (2018), no. 3 215, [arXiv:1707.09036].

[5] **MSSM Working Group** Collaboration, A. Djouadi et al., *The Minimal supersymmetric standard model: Group summary report*, in *GDR (Groupement De Recherche) - Supersymetrie, Montpellier, France, April 15-17, 1998.* hep-ph/9901246.

[6] http://hepdata.cedar.ac.uk/view/ins1389857.

[7] **ATLAS** Collaboration, G. Aad et al., *Summary of the ATLAS experiment's sensitivity to supersymmetry after LHC Run 1 interpreted in the phenomenological MSSM*, *JHEP* **10** (2015) 134, [arXiv:1508.06608].

[8] F. Ambrogi, S. Kraml, S. Kulkarni, U. Laa, A. Lessa, V. Magerl, J. Sonneveld, M. Traub, and W. Waltenberger, *SModelS v1.1 user manual: Improving simplified model constraints with efficiency maps*, *Comput. Phys. Commun.* **227** (2018) 72–98, [arXiv:1701.06586].

[9] J. Alwall, M. Herquet, F. Maltoni, O. Mattelaer, and T. Stelzer, *MadGraph 5 : Going Beyond*, *JHEP* **06** (2011) 128, [arXiv:1106.0522].

[10] T. Sjostrand, S. Mrenna, and P. Z. Skands, *PYTHIA 6.4 Physics and Manual*, *JHEP* **0605** (2006) 026, [hep-ph/0603175].

[11] S. Hoeche, F. Krauss, N. Lavesson, L. Lonnblad, M. Mangano, A. Schalicke, and S. Schumann, *Matching parton showers and matrix elements*, in *HERA and the LHC: A Workshop on the implications of HERA for LHC physics: Proceedings Part A*, pp. 288–289, 2005. hep-ph/0602031.

[12] J. Alwall et al., *Comparative study of various algorithms for the merging of parton showers and matrix elements in hadronic collisions*, *Eur. Phys. J.* **C53** (2008) 473–500, [arXiv:0706.2569].

[13] G. Chalons and D. Sengupta, *Madanalysis 5 implementation of the ATLAS multi jet analysis documented in arXiv:1405.7875*, *JHEP* 1409 (2014) 176, .

[14] https://madanalysis.irmp.ucl.ac.be/raw-attachment/wiki/PublicAnalysisDatabase/ma5_atlas_1405_7875.pdf.

[15] S. Bein and D. Sengupta, *MadAnalysis 5 implementation of CMS-SUS-13-012*, .

[16] http://madanalysis.irmp.ucl.ac.be/raw-attachment/wiki/PublicAnalysisDatabase/ma5_validation_CMS-SUS-13-012.pdf.

[17] M. Cacciari, G. P. Salam, and G. Soyez, *FastJet User Manual*, *Eur.Phys.J.* **C72** (2012) 1896, [arXiv:1111.6097].

[18] S. Kraml, S. Kulkarni, U. Laa, A. Lessa, W. Magerl, D. Proschofsky-Spindler, and W. Waltenberger, *SModelS: a tool for interpreting simplified-model results from the LHC and its application to supersymmetry*, *Eur. Phys. J.* **C74** (2014) 2868, [arXiv:1312.4175].

[19] F. Ambrogi et al., *SModelS v1.2: long-lived particles, combination of signal regions, and other novelties*, arXiv:1811.10624.

[20] A. L. Read, *Presentation of search results: The CL(s) technique*, *J. Phys.* **G28** (2002) 2693–2704. [,11(2002)].

[21] T. Junk, *Confidence level computation for combining searches with small statistics*, *Nucl. Instrum. Meth.* **A434** (1999) 435–443, [hep-ex/9902006].

[22] P. Z. Skands et al., *SUSY Les Houches accord: Interfacing SUSY spectrum calculators, decay packages, and event generators*, *JHEP* **07** (2004) 036, [hep-ph/0311123].

[23] C. F. Berger, J. S. Gainer, J. L. Hewett, and T. G.

Rizzo, *Supersymmetry Without Prejudice*, *JHEP* **02** (2009) 023, [arXiv:0812.0980].

[24] M. W. Cahill-Rowley, J. L. Hewett, S. Hoeche, A. Ismail, and T. G. Rizzo, *The New Look pMSSM with Neutralino and Gravitino LSPs*, *Eur. Phys. J.* **C72** (2012) 2156, [arXiv:1206.4321].

[25] M. W. Cahill-Rowley, J. L. Hewett, A. Ismail, and T. G. Rizzo, *More energy, more searches, but the phenomenological MSSM lives on*, *Phys. Rev.* **D88** (2013), no. 3 035002, [arXiv:1211.1981].

[26] M. Cahill-Rowley, J. L. Hewett, A. Ismail, and T. G. Rizzo, *Lessons and prospects from the pMSSM after LHC Run I*, *Phys. Rev.* **D91** (2015), no. 5 055002, [arXiv:1407.4130].

[27] S. P. Martin, *A Supersymmetry primer*, hep-ph/9709356. [Adv. Ser. Direct. High Energy Phys.18,1(1998)].

[28] T. Sjostrand, S. Ask, J. R. Christiansen, R. Corke, N. Desai, P. Ilten, S. Mrenna, S. Prestel, C. O. Rasmussen, and P. Z. Skands, *An Introduction to PYTHIA 8.2*, *Comput. Phys. Commun.* **191** (2015) 159–177, [arXiv:1410.3012].

[29] http://pauli.uni-muenster.de/~akule_01/nllwiki/index.php/NLL-fast.

[30] W. Beenakker, R. Hopker, M. Spira, and P. Zerwas, *Squark and gluino production at hadron colliders*, *Nucl.Phys.* **B492** (1997) 51–103, [hep-ph/9610490].

[31] A. Kulesza and L. Motyka, *Threshold resummation for squark-antisquark and gluino-pair production at the LHC*, *Phys.Rev.Lett.* **102** (2009) 111802, [arXiv:0807.2405].

[32] A. Kulesza and L. Motyka, *Soft gluon resummation for the production of gluino-gluino and squark-antisquark pairs at the LHC*, *Phys.Rev.* **D80** (2009) 095004, [arXiv:0905.4749].

[33] W. Beenakker, S. Brensing, M. Kramer, A. Kulesza, E. Laenen, et al., *Soft-gluon resummation for squark and gluino hadroproduction*, *JHEP* **0912** (2009) 041, [arXiv:0909.4418].

[34] W. Beenakker, S. Brensing, M. Kramer, A. Kulesza, E. Laenen, et al., *Squark and Gluino Hadroproduction*, *Int.J.Mod.Phys.* **A26** (2011) 2637–2664, [arXiv:1105.1110].

[35] W. Beenakker, M. Kramer, T. Plehn, M. Spira, and P. Zerwas, *Stop production at hadron colliders*, *Nucl.Phys.* **B515** (1998) 3–14, [hep-ph/9710451].

[36] W. Beenakker, S. Brensing, M. Kramer, A. Kulesza, E. Laenen, et al., *Supersymmetric top and bottom squark production at hadron colliders*, *JHEP* **1008** (2010) 098, [arXiv:1006.4771].

[37] http://fastlim.web.cern.ch/.

[38] https://github.com/SModelS/smodels-database-release/releases/.

[39] S. Kraml, U. Laa, L. Panizzi, and H. Prager, *Scalar versus fermionic top partner interpretations of $t\bar{t} + E_T^{\mathrm{miss}}$ searches at the LHC*, *JHEP* **11** (2016) 107, [arXiv:1607.02050].

[40] J. Dutta, S. Kraml, A. Lessa, and W. Waltenberger, *SModelS extension with the CMS supersymmetry search results from Run 2*, *LHEP* **1** (2018), no. 1 5–12, [arXiv:1803.02204].

Appendix A. Limits Comparison

The following Tables A.6 and A.7 compare the upper limits obtained for the mass point $(M_1, M_2, M_3) = (1000, 200, 190), (1200, 600, 500)$ GeV for the two different hierarchy models $T3GQ(m_{\tilde{g}}, m_{\tilde{q}}, m_{\tilde{\chi}_1^0})$ and $T3QG(m_{\tilde{q}}, m_{\tilde{g}}, m_{\tilde{\chi}_1^0})$. In bold, the best SR providing the strongest expected limit and corresponding observed limit is shown. The difference in the efficiency and consequent choice of a different SR, respectively *2jm* for *T3GQ* and *2jt* for *T3QG*, favours a strongest limit for the *T3GQ* case. However the difference is contained within a factor 2, which translates to only few tens of GeV difference in the excluded mass of Squarks or Gluinos. The value of the observed UL, quoted by `SModelS`, is indicated with an asterisk.

$(M_1, M_2, M_3) = (1000, 200, 190)$				**T3GQ**			**T3QG**	
SR	UL_{exp}	UL_{obs}	ϵ	UL_{exp}/ϵ	UL_{obs}/ϵ	ϵ	UL_{exp}/ϵ	UL_{obs}/ϵ
2jm	5.552	4.242	0.118	**47.1**	**36.0**	0.090	**61.5***	**47.0***
2jt	1.512	1.818	0.032	**47.9**	**57.5**	0.027	**56.1**	**67.4**
3j	0.332	0.433	0.002	139.4	182.2	0.002	186.4	243.6
4jl	5.435	4.749	0.032	171.4	149.8	0.039	139.7	122.1
4jl-	11.561	13.292	0.036	318.7	366.4	0.047	248.0	285.2
4jt	0.240	0.149	0.002	146.1	90.8	0.001	178.1	110.8
5j	1.714	1.543	0.007	245.1	220.7	0.010	172.9	155.6
6jl	1.531	1.923	0.002	965.5	1212.5	0.003	555.5	697.7
6jt	0.333	0.332	0.001	472.8	470.4	0.001	327.8	326.2
6jt+	0.302	0.399	0.001	428.6	566.3	0.001	297.2	392.7

Table A.6: Summary of the UL for the SRs of ATLAS-SUSY-2013-02, for the *T3GQ* and *T3QG* models, with mass spectrum $(M_1, M_2, M_3) = (1000, 200, 190)$ GeV. In bold, the expected and observed limits for the best SRs are highlighted. With a star, the value of the observed UL used by `SModelS` is indicated.

$(M_1, M_2, M_3) = (1200, 600, 500)$				**T3GQ**			**T3QG**	
SR	UL_{exp}	UL_{obs}	ϵ	UL_{exp}/ϵ	UL_{obs}/ϵ	ϵ	UL_{exp}/ϵ	UL_{obs}/ϵ
2jm	5.552	4.242	0.178	31.172	23.815	0.184	30.111	23.004
2jt	1.512	1.818	0.061	**24.623**	**29.601**	0.069	**21.949***	**26.385***
3j	0.332	0.433	0.005	61.421	80.255	0.005	64.971	84.893
4jl	5.435	4.749	0.165	69.892	80.356	0.188	61.542	70.756
4jl-	11.561	13.292	0.145	37.596	32.851	0.166	32.813	28.672
4jt	0.240	0.149	0.004	54.035	33.611	0.004	54.765	34.065
5j	1.714	1.543	0.048	36.043	32.449	0.055	31.004	27.912
6jl	1.531	1.923	0.016	98.361	123.530	0.018	83.039	104.286
6jt	0.333	0.332	0.008	43.713	43.489	0.007	45.136	44.905
6jt+	0.302	0.399	0.008	39.632	52.359	0.007	40.922	54.063

Table A.7: Summary of the UL for the SRs of ATLAS-SUSY-2013-02, for the *T3GQ* and *T3QG* models, with mass spectrum $(M_1, M_2, M_3) = (1200, 600, 500)$ GeV. In bold, the expected and observed limits for the best SR are highlited.
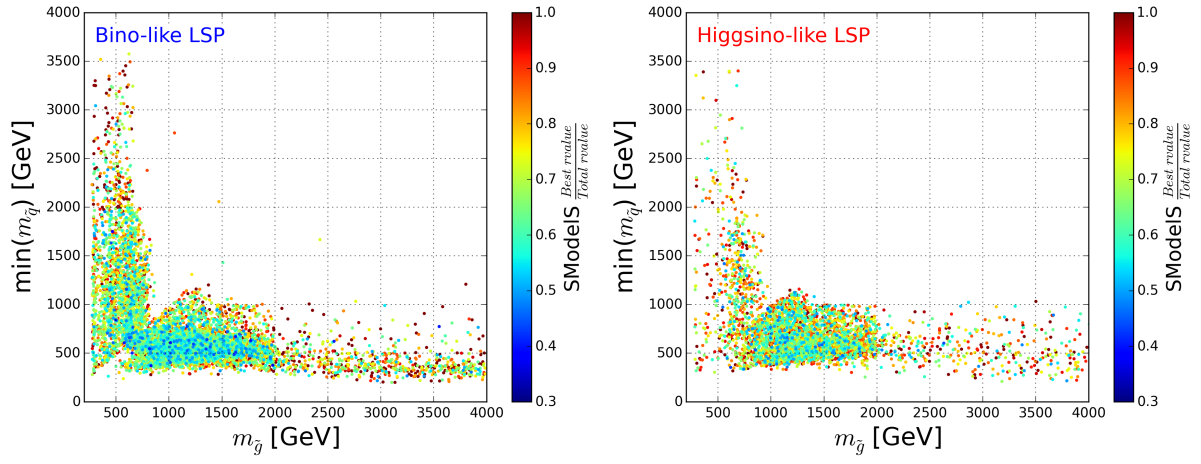
Extra material

Figure A.10: Fractional contribution of the model with the highest r value to the total rvalue. Points in dark blue benefit from the combination of the three signals for *T2*, *T5* and *T3GQ*, meaning that the each largest contribution from a single signal reaches up to $\sim 40\%$ of the total signal.